



Otolithic Receptor Mechanisms for Vestibular-Evoked Myogenic Potentials: A Review

Ian S. Curthoys^{1*}, J. Wally Grant², Ann M. Burgess¹, Chris J. Pastras³, Daniel J. Brown³ and Leonardo Manzari⁴

¹Vestibular Research Laboratory, School of Psychology, The University of Sydney, Sydney, NSW, Australia, ²Department of Biomedical Engineering and Mechanics, VA Tech, Blacksburg, VA, United States, ³The Menière's Laboratory, Sydney Medical School, The University of Sydney, Sydney, NSW, Australia, ⁴MSA ENT Academy Center, Cassino, Italy

OPEN ACCESS

Edited by:

Brian D. Corneil,
University of Western Ontario,
Canada

Reviewed by:

Mathieu Beraneck,
UMR8119 Centre de neurophysique,
physiologie, pathologie, France
Erin Gillikin Piker,
James Madison University,
United States

*Correspondence:

Ian S. Curthoys
ian.curthoys@sydney.edu.au

Specialty section:

This article was submitted to
Neuro-Otology,
a section of the journal
Frontiers in Neurology

Received: 26 March 2018

Accepted: 07 May 2018

Published: 25 May 2018

Citation:

Curthoys IS, Grant JW, Burgess AM,
Pastras CJ, Brown DJ and Manzari L
(2018) Otolithic Receptor
Mechanisms for Vestibular-Evoked
Myogenic Potentials: A Review.
Front. Neurol. 9:366.
doi: 10.3389/fneur.2018.00366

Air-conducted sound and bone-conducted vibration activate otolith receptors and afferent neurons in both the utricular and saccular maculae, and trigger small electro-myographic (EMG) responses [called vestibular-evoked myogenic potentials (VEMPs)] in various muscle groups throughout the body. The use of these VEMPs for clinical assessment of human otolith function is built on the following logical steps: (1) that high-frequency sound and vibration at clinically effective stimulus levels activate otolith receptors and afferents, rather than semicircular canal afferents, (2) that there is differential anatomical projection of otolith afferents to eye muscles and neck muscles, and (3) that isolated stimulation of the utricular macula induces short latency responses in eye muscles, and that isolated stimulation of the saccular macula induces short latency responses in neck motoneurons. Evidence supports these logical steps, and so VEMPs are increasingly being used for clinical assessment of otolith function, even differential evaluation of utricular and saccular function. The proposal, originally put forward by Curthoys in 2010, is now accepted: that the ocular vestibular-evoked myogenic potential reflects predominantly contralateral utricular function and the cervical vestibular-evoked myogenic potential reflects predominantly ipsilateral saccular function. So VEMPs can provide differential tests of utricular and saccular function, not because of stimulus selectivity for either of the two maculae, but by measuring responses which are predominantly determined by the differential neural projection of utricular as opposed to saccular neural information to various muscle groups. The major question which this review addresses is how the otolith sensory system, with such a high density otoconial layer, can be activated by individual cycles of sound and vibration and show such tight locking of the timing of action potentials of single primary otolith afferents to a particular phase angle of the stimulus cycle even at frequencies far above 1,000 Hz. The new explanation is that it is due to the otoliths acting as seismometers at high frequencies and accelerometers at low frequencies. VEMPs are an otolith-dominated response, but in a particular clinical condition, semicircular canal dehiscence, semicircular canal receptors are also activated by sound and vibration, and act to enhance the otolith-dominated VEMP responses.

Keywords: vestibular, utricular, saccular, vestibular-evoked myogenic potential, cervical vestibular-evoked myogenic potential, ocular vestibular-evoked myogenic potential, sound, vibration

PREFACE

In the last 5 years, there has been a very rapid growth of knowledge concerning vestibular-evoked myogenic potentials (VEMPs) and their physiological basis (1, 2). This includes new understanding of how sound and vibration activate otolithic receptors. The present review seeks to provide a concise comprehensive overview, as accurate as we can make it at May 2018, of the basic physiological mechanisms underlying VEMPs.

INTRODUCTION

Before the 1990s, the usual way to probe the function of the otoliths was to measure responses, such as eye movements or perception, to maintained or low-frequency linear acceleration stimuli provided by sleds or centrifuges or tilting chairs (3–8). Such tests were clinically impractical because of the small, variable, unreliable responses, as well as safety issues in delivering the stimuli. Since then there has been a major change: now surface electrodes on the skin are being used to record myogenic potentials in response to sound and vibration to probe otolith function, simply, quickly, reliably, and safely. These are called vestibular-evoked myogenic potentials (VEMPs). It is now clear that because of extensive indirect projections of vestibular neurons there are a host of VEMPs throughout the body (9, 10), with the two most frequently studied being the cervical vestibular-evoked myogenic potential [cVEMP—recorded from above the tensed sternocleidomastoid muscle (SCM)] and the ocular vestibular-evoked myogenic potential (oVEMP—recorded from above the inferior oblique as the patient looks up) (11–14) (see **Figure 1**).

The primary question is: are VEMP responses to sound (ACS) or bone-conducted vibration (BCV) really due to vestibular activation, since obviously sound and vibration stimulate cochlear receptors? That question was answered by showing the presence of VEMPs in patients without hearing but with vestibular function, and the absence of VEMPs in patients with hearing but without vestibular function after systemic gentamicin (11, 13, 17). These data show conclusively that VEMP tests are vestibular and not cochlear, and that evidence is supported by physiological research showing primary otolithic neurons are activated by sound and vibration. However, the next major question is how sound and vibration activate otolithic receptors and afferents, and that is the main focus of this review—the physiological basis for using these myogenic potentials to index otolith function, and the rationale for using these tests to test utricular or saccular function differentially.

The traditional view of the otoliths has been that they are flat sheets of tissue (called maculae—**Figure 2**) in which there are

embedded thousands of receptor hair cells with their hair bundles projecting into the gelatinous otoconial layer (OL) covered by crystals of dense otoconia [specific gravity of 2.73—similar to granite (18)]. In the human, there are around 33,000 receptors in each utricular macula and 18,000 in each saccular macula, with about 5,000 utricular afferents and 4,000 saccular afferents (19, 20). The stimulus for causing vestibular hair cell transduction is deflection of the hair bundle with respect to the cell body of the receptor in the neuroepithelial layer (NEL) of the macula or crista. The traditional view is that the otoliths are stimulated by linear accelerations (such as head tilt) because the linear acceleration drags the otoconia and so deflects the hair bundles of the otolithic receptors (21) (**Figures 2B–E**). Because of the high density of the otoconia, the otoliths have been regarded as a sensory system responsive to static tilts and fairly low frequencies of linear acceleration—up to a few hundred Hertz [e.g., Ref. (21–26)].

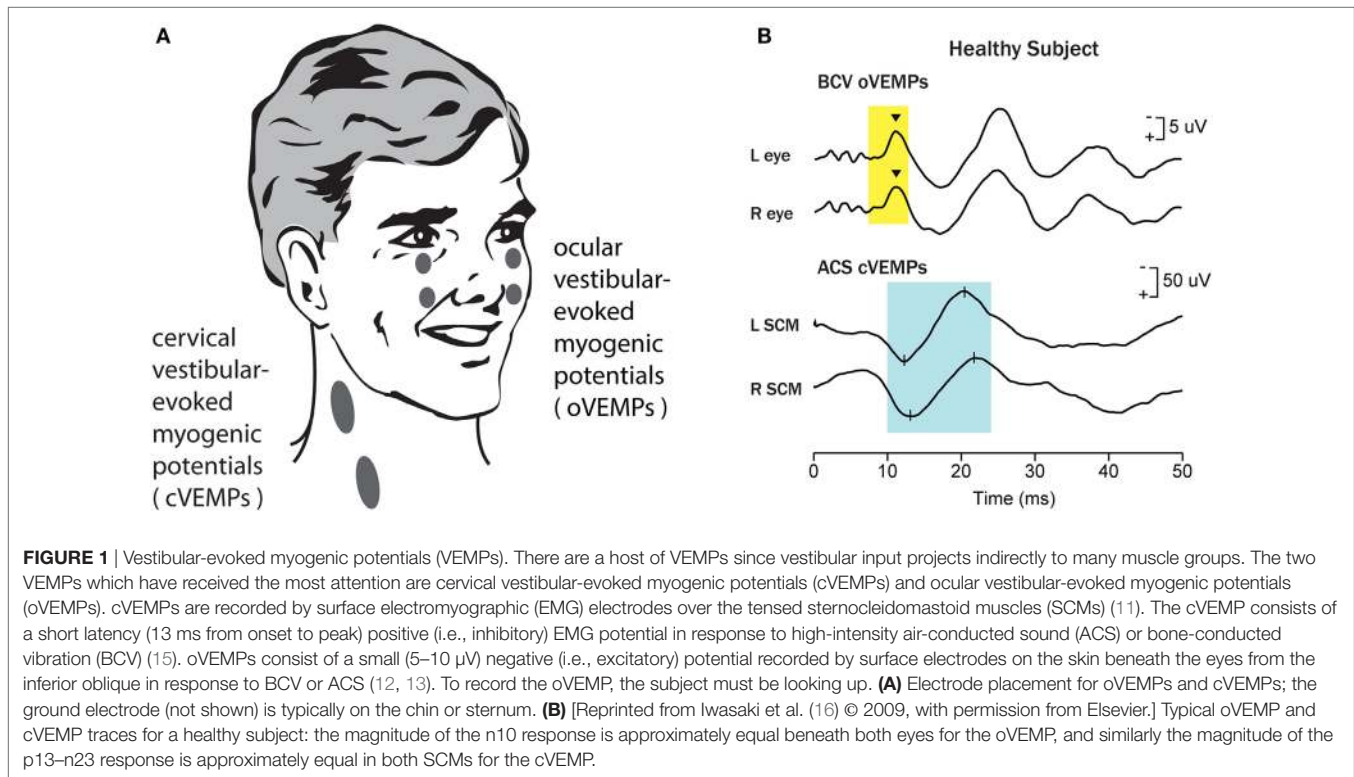
Physiological evidence shows the otoliths do respond to maintained tilts and low-frequency linear accelerations, and here, we call this the accelerometer mode of otolith operation. But there is now abundant evidence that some otolithic receptors and afferents can be activated by air-conducted sound (ACS) and BCV up to frequencies of thousands of Hertz. This is shown by neural recordings of otolithic afferents with irregular resting discharge in squirrel monkey, cat, rat, and guinea pig (28–41). This neural evidence of otolithic activation by high frequencies is the foundation on which VEMPs to ACS and BCV are used to test otolith function.

The maculae are (moderately) curved structures (**Figure 2**) (42). The receptor cells, embedded in the neuroepithelium of the maculae, fall into two types: amphora-shaped type I receptors or cylindrical type II receptors, and these two types are intermingled across the maculae (43, 44). Otolithic receptors are activated by hair bundle deflection toward the longest cilium (the kinocilium), and so each receptor has a preferred direction which is termed its morphological polarization. The receptors have opposite morphological polarization on either side of a dividing line now called “the line of polarity reversal” (**Figure 2**).

The receptors in a band (called the striola) straddling the line of polarity reversal are especially important—they have short stiff cilia with tenuous attachment to the otoconial membrane (27, 45), and there is a greater concentration of type I receptors in the striola (44, 46). The type I receptor cell bodies are enveloped by the calyx ending of afferents with irregular resting discharge (31, 47, 48). It appears that the attachment of the hair bundles of striolar receptors to the overlying otoconial membrane is tenuous (27, 49, 50). Extracellular recordings from primary otolithic afferents with irregular resting discharge have shown that these afferents are sensitive to sound and vibration, and histological tracing has shown these afferents contact type I receptors at the striola (31, 33).

Songer and Eatock (51) used intracellular recording from isolated type I otolithic receptors and showed that mammalian type I receptors could respond to displacements at frequencies of hundreds of Hertz (and probably higher). The size of these displacements is small, but only small displacements are needed since individual vestibular receptors are almost as sensitive as individual cochlear receptors. Using intracellular recordings

Abbreviations: ABR, auditory brainstem response; ACS, air-conducted sound; BCV, bone-conducted vibration; Fz, the midline of forehead at the hairline; IO, inferior oblique eye muscle; VEMP, vestibular-evoked myogenic potential; cVEMP, cervical vestibular-evoked myogenic potential; oVEMP, ocular vestibular-evoked myogenic potential; OL, otoconial layer; NEL, neuroepithelial layer; SCD, semicircular canal dehiscence; n10, the negative potential of the oVEMP at about 10 ms latency; SCM, sternocleidomastoid muscle; SPL, sound pressure level.



from individual receptors stimulated by hair bundle deflection, Geleoc et al. (52) have shown that isolated vestibular receptors have similar thresholds for hair bundle displacement as cochlear receptors—deflections of the receptor hair bundles of around 10 nm generate intracellular potentials in both cochlear and vestibular receptors.

Throughout both utricular and saccular maculae, there are receptors (probably cylindrical type II receptors) with long cilia projecting into the otolithic membrane (45). Afferent neurons with regular resting discharge make extensive contacts with extrastricular type I and II receptors (47), but guinea pig otolithic afferents with regular resting discharge do not respond to ACS and BCV at reasonable levels [2 g peak to peak max or 130 dB sound pressure level (SPL) (31)].

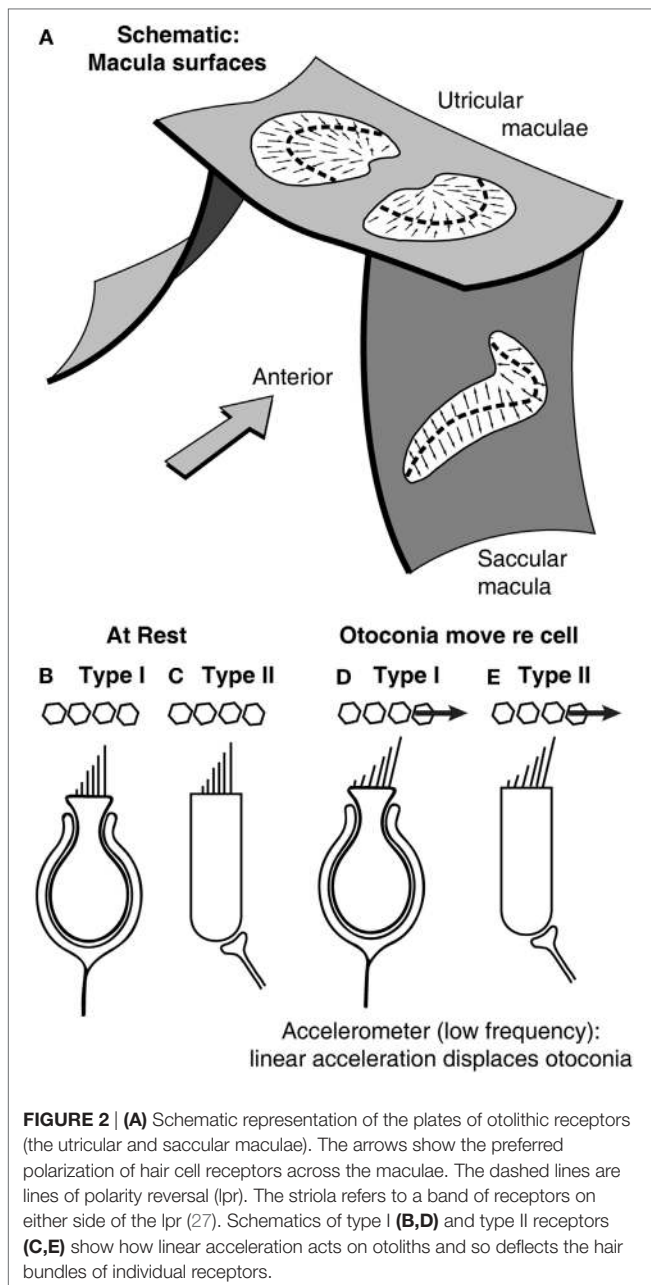
Extracellular recordings of single primary otolithic afferents with irregular resting discharge show that they have a stimulus-locked increase in firing rate to ACS or BCV stimulation up to frequencies of thousands of Hertz (31) (Figure 3). The threshold as a function of frequency is very different for ACS vs BCV. For ACS, the lowest thresholds are at around 90 dB SPL at 1,000 Hz, with cells still responding with relatively low thresholds to 2,000 and 3,000 Hz ACS stimuli. For BCV, the lowest threshold is around 0.02 g at frequencies from 100 to 500 Hz. For BCV frequencies above 750 Hz, there is a very steep increase in threshold beyond 750 Hz, so that few neurons are activated by BCV at 2,000 Hz (even at 2 g peak to peak). At lower frequencies such as 500 and 750 Hz, BCV is a much more effective and reliable stimulus than ACS—the threshold for single neurons to BCV is around 0.02 g peak to peak, which is around the level for auditory brainstem

response (ABR) threshold, whereas vestibular neural thresholds for ACS are at levels about 70 dB above ABR threshold (29, 31).

PHASE LOCKING

The exact response of these primary otolithic irregular neurons to BCV and ACS reveals a vital principle in the mechanism of transduction of high frequencies. For all neurons activated by ACS or BCV, the neurons do not fire an action potential on every single cycle, but the moment when the neuron fires is locked to a narrow band of phase angles of the stimulus waveform (Figure 4) (31, 38, 53). This is true up to very high frequencies even >3,000 Hz. For individual afferents, the measured optimum phase angle systematically changes with frequency for both ACS and BCV, reflecting the latency of the afferent. Also the optimum phase angle for an individual afferent neuron at a given frequency is not constant but varies from neuron to neuron (38, 53).

The phenomenon of phase locking shows that for both BCV and ACS, every single cycle of the sine wave stimulus is the effective stimulus for the afferent (31), even up to frequencies of 3,000 Hz where the duration of an individual cycle is so short (0.3 ms). It means that the receptors are being displaced at this very high frequency (3,000 times/s in this example), but when they fire is tightly locked to a particular phase angle of the sine wave stimulus even at this high frequency (38). Phase locking is very well established for cochlear receptors and afferents—the action potentials in cochlear afferent neurons are locked to each displacement of the basilar membrane. Phase locking of cochlear afferents is recognized as being a major code for the transmission



of auditory frequency information (54, 55), see Fettiplace (56) for a recent excellent review. It is now clear that phase locking applies to otolithic neurons with very tight locking to particular phase angles up to high frequencies. This may be due to the fact that irregular afferents are excellent detectors of change in stimulation (jerk detectors) (31, 38).

How can such an apparently sluggish system as the otoliths with such dense otoconia exhibit phase locking to stimulus frequencies of thousands of Hertz? One answer comes from recording the vestibular microphonic, which shows that mammalian utricular receptors are activated at such high frequencies (57, 58). The vestibular microphonic is a field potential to sound or vibration and is a direct electrophysiological indicator

of otolithic receptor hair cell function. The vestibular microphonic has been recorded *in vivo* in anesthetized guinea pigs by electrodes piercing the underside of the utricular macula with a glass microelectrode and then measuring the vestibular microphonic to BCV or ACS stimuli of varying frequency and amplitude (Figure 5) (57). Most importantly, in these animals, the cochlea has been completely removed, so there is no contribution from the cochlear microphonic. The recent paper (57) gives the evidence that the vestibular microphonic is a field potential due to otolithic receptor hair cell activation—reporting all the correct controls—such as chemically silencing afferent neurons and showing that the vestibular microphonic remains, and conversely chemically silencing the receptors and showing that the vestibular microphonic disappears, leading to the conclusion that the vestibular microphonic is a field potential generated by otolithic hair cells (utricular hair cells in this case) (Figure 5). The vestibular microphonic (strictly the utricular microphonic) has been recorded up to frequencies of 3,000 Hz. Those results complement the results from single neuron recordings: mammalian utricular receptors really do respond to very high frequencies (up to 3,000 Hz), far above what the otoliths are usually thought to be capable of transducing. But how? The simple answer is that the macula moves.

Many years ago, Tullio used fine aluminum particles on the surface of the utricular macula to demonstrate visually that sound caused rabbit utricular macula to move (60). We have confirmed Tullio's results by using laser Doppler vibrometry to measure the velocity of guinea pig utricular macula movement during ACS and BCV stimulation. A tiny glass bead was placed on the exposed underside of the utricular macula and a laser beam aimed at it. The Doppler shift in the wavelength of the reflected beam during BCV or ACS stimulation (59) confirms that the macula is moving and gives the macula velocity. These measures show that both ACS and BCV cause the macula to move as Tullio had reported, and at frequencies up to 3,000 Hz. The actual displacements are small—nanometers—but the results of Geleoc et al. (52) show how very sensitive vestibular receptors are, so that deflections of the macula of nanometers can activate vestibular receptors.

Irregular otolithic afferents respond to the time rate of change of acceleration (jerk) rather than to acceleration itself. That jerk sensitivity has been demonstrated in otolithic evoked potentials (61) to pulses of linear acceleration. That jerk sensitivity adds to the puzzle—now this “sluggish” system not only transduces maintained linear accelerations but also this evidence shows it really does respond to extremely fast stimuli. The puzzle to be explained is that the one sensory system is responding over a large range of frequencies—from DC up to 3,000 Hz. How could high frequencies of BCV cause macula and hair bundle displacements at 3,000 Hz, given the very large specific gravity of the otoconia and the viscosity of the otolithic membrane?

Grant and Curthoys (62) have put forward a model of the otoliths which addresses that question. The model holds that there are two modes of otolithic operation: the traditional accelerometer mode and the new seismometer mode. At low frequencies of BCV, the otoconia move relative to the skull, while the macula stays stationary, and so the hair bundles of the receptor cells

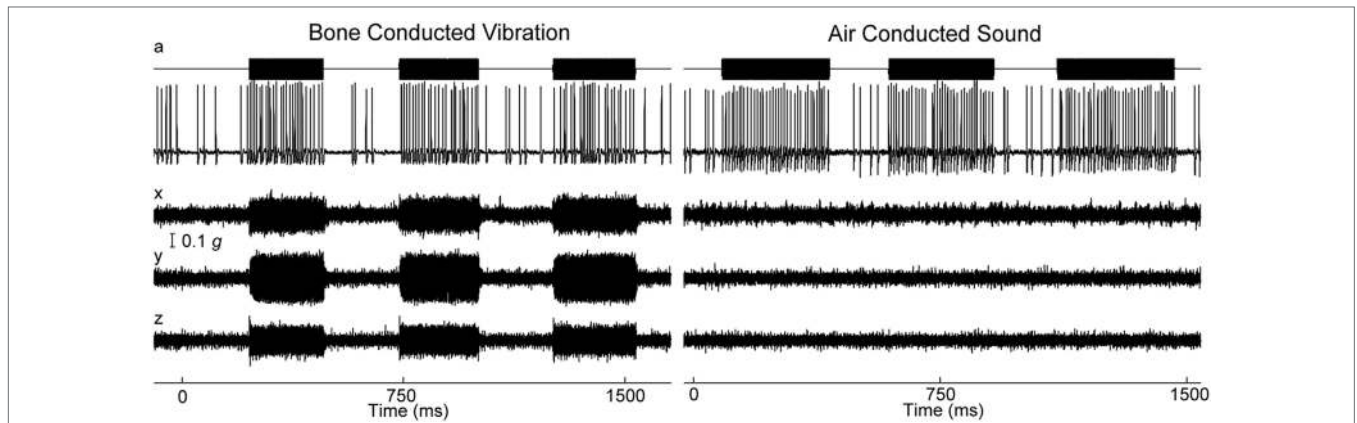


FIGURE 3 | Time series of firing of an irregular otolith neuron during stimulation by bone-conducted vibration (BCV) and air-conducted sound (ACS) at 500 Hz—both stimuli cause stimulus-locked activation. The top trace (a) shows the command voltage indicating when the stimulus is on. The second trace shows the extracellular recording. The three bottom traces (x, y, z) show the triaxial accelerometer recording of the stimulus. The *left panel* is an example of BCV stimulation and the *right* of ACS stimulation of the same neuron. Note the scale of stimulus intensity in g at the left margin between traces x and y. Reprinted by permission from Springer Nature, Curthoys and Vulovic (29), © 2011.

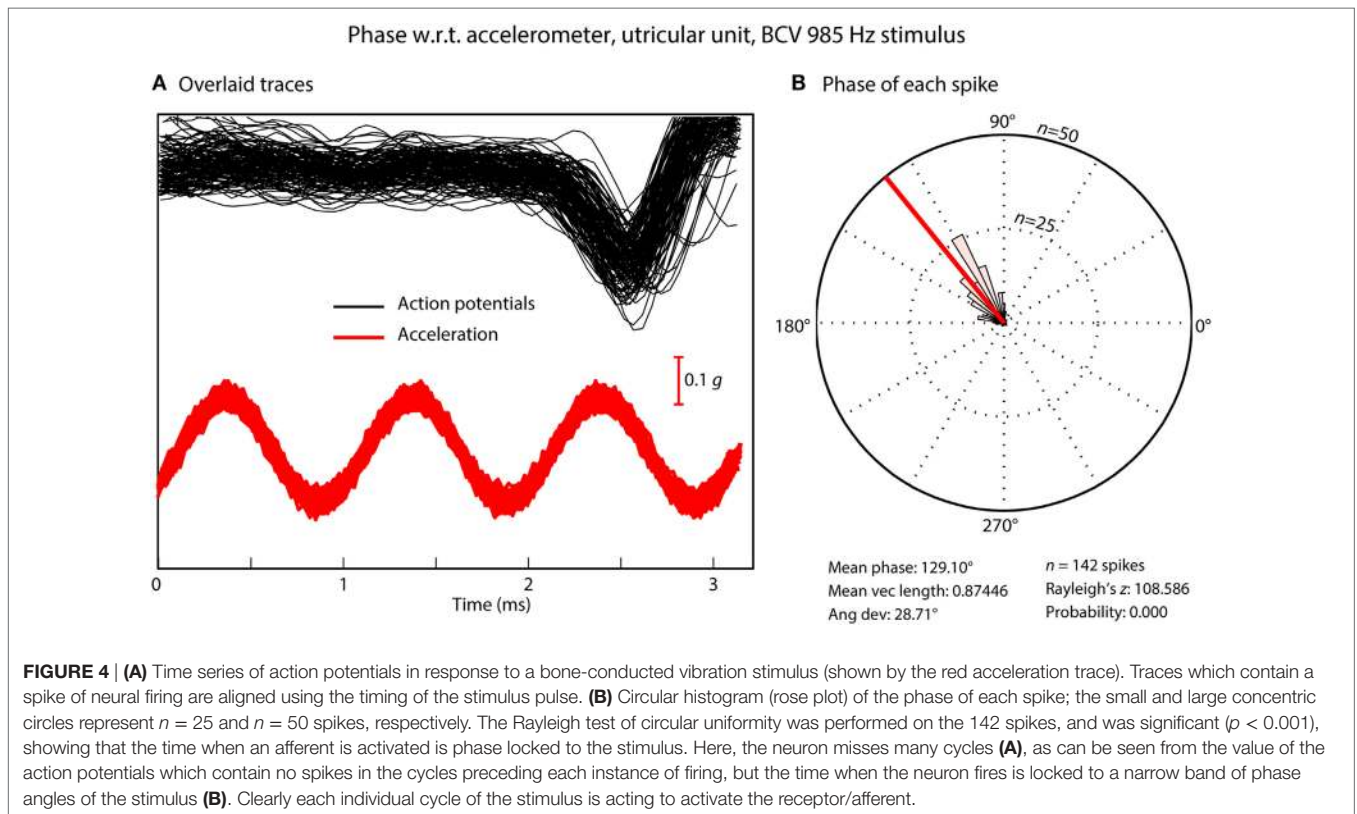
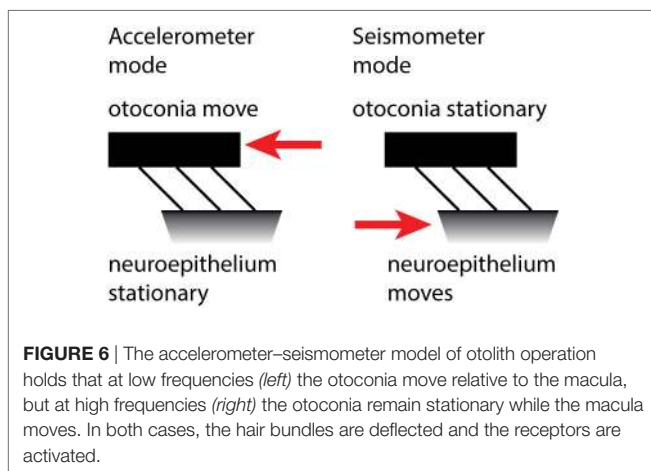
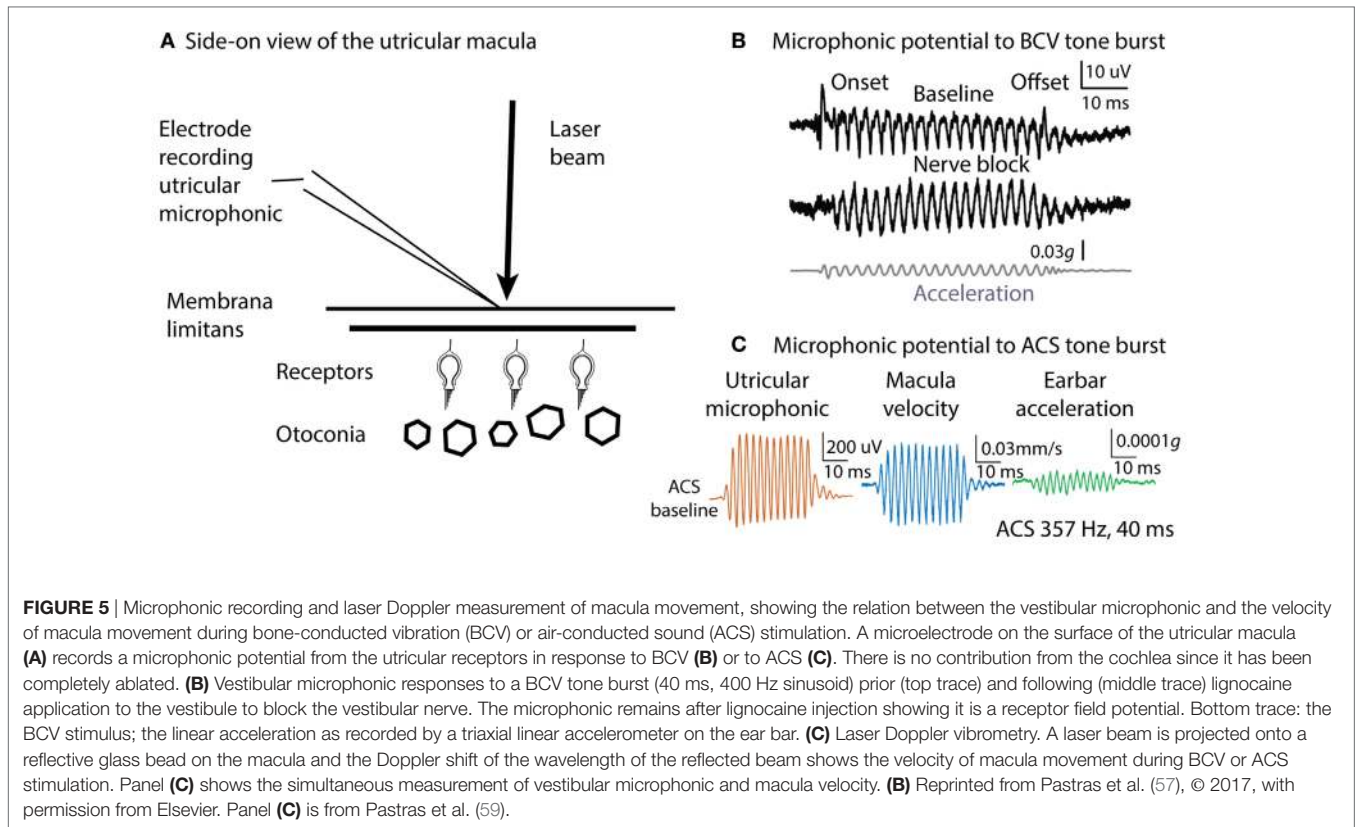


FIGURE 4 | **(A)** Time series of action potentials in response to a bone-conducted vibration stimulus (shown by the red acceleration trace). Traces which contain a spike of neural firing are aligned using the timing of the stimulus pulse. **(B)** Circular histogram (rose plot) of the phase of each spike; the small and large concentric circles represent $n = 25$ and $n = 50$ spikes, respectively. The Rayleigh test of circular uniformity was performed on the 142 spikes, and was significant ($p < 0.001$), showing that the time when an afferent is activated is phase locked to the stimulus. Here, the neuron misses many cycles **(A)**, as can be seen from the value of the action potentials which contain no spikes in the cycles preceding each instance of firing, but the time when the neuron fires is locked to a narrow band of phase angles of the stimulus **(B)**. Clearly each individual cycle of the stimulus is acting to activate the receptor/afferent.

are deflected (**Figure 6**). This is the “traditional” accelerometer mode of operation. In the accelerometer mode, the otoconia move relative to the macula, while the macula is accelerated with the skull motion. At high frequencies, the system operates in the seismometer mode: the otoconia remain at rest (due to their inertia) while the macula is in motion, again producing a relative displacement between the otoconia and macula. In both

cases, there is relative motion between the otoconia and macula, displacing hair bundles. We explain this in more detail below.

Otoliths are biological–mechanical sensors that measure the acceleration of the head in the plane of the otolith. The acceleration that is measured is the vector sum of gravity and the inertial acceleration and is called the gravito-inertial acceleration, but is generally just referred to as the head acceleration. The otolith



acceleration value is a measurement of the relative displacement between the otolithic membrane and the NEL. This displacement measurement is made by the hair cells in the NEL and reported to the brain *via* the otolithic afferents.

Static or low-frequency linear acceleration causes the otoconia to move relative to the NEL of the utricular macula. During a maintained head tilt (a DC stimulus), the linear acceleration of gravity acts on the otoconia and displaces the otoconia relative to the NEL, so the hair bundles of the otolithic receptor hair cells (both type I and type II receptors) are deflected relative to their cell bodies and a neural signal is transmitted to the brain

via the otolithic afferents, signaling that linear acceleration has occurred. This is the “traditional” accelerometer mode of otolith operation.

If a high-frequency vibration (e.g., 2,000 Hz) is applied to the skull, it causes the NEL to move at the same 2,000 Hz frequency. But because of their mass, the otoconia remain stationary. The consequence is that again the hair bundles will be deflected and action potentials will be propagated in otolithic afferent neurons. This is the seismometer mode of otolith operation. The difference is that in the first (accelerometer) mode, the otoconia move relative to the skull and in the second (seismometer) mode, the macula moves relative to the skull. In both modes, the otoconia and macula move with respect to each other, so the hair bundles of the receptors are displaced relative to the cell body. In this way, linear acceleration and high-frequency vibration can both stimulate the otolithic receptors.

Neurons cannot fire at such high rates (2,000 spikes/s), but at all frequencies the hair bundles of the receptors are deflected and activated once per cycle, and the neural evidence shows that when the afferent neurons fire, the action potentials show phase locking to the individual cycles of the stimulus at both low and high frequencies.

Given the usual stimulus strength used in VEMP testing to BCV, we estimate that the magnitude of these deflections is probably in the 50–80 nm range. With such small deflections, it is only the type I hair cells in the striolar region, that are stimulated. These type I hair cells are stiff (45) due to their large number of stereocilia and are stimulated with these small

displacements seen in the high-frequency seismometer mode stimulus. The type II hair cells are less stiff and require larger deflections for stimulation. Afferents with regular resting discharge receive input predominantly from type II receptors, but are not activated by high-frequency BCV or ACS at the levels tested experimentally.

The model is essentially the result of application of engineering principles for the design of accelerometers and seismometers, to the otoliths. Importantly, engineering analysis shows that the one system can operate both as an accelerometer and as a seismometer. On this “accelerometer–seismometer” model, the one sensory system, the otoliths, transduces both low-frequency (even DC) linear accelerations and also very high-frequency stimuli. The empirical evidence that this happens comes from recordings of single otolithic afferents to a wide range of frequencies varying from 37 to 2,000 Hz (31) and showing that the one afferent is activated by stimuli across such a large frequency range, and from measuring (and modeling) the stimulus thresholds needed to activate the neuron across this large range.

Commercial accelerometers have an undamped natural frequency in the 10–20 kHz range and seismometers in the 5–10 Hz range. Otoliths have undamped natural frequencies in between these frequencies, which allows them to operate in both modes (accelerometer and seismometer) over the frequency ranges that have been shown to activate otoliths. It is the unique undamped natural frequency that allows the otoliths to make the transition over the two operating modes.

While this model accounts for the fact that receptor hair bundles can be displaced at various frequencies, we need to drill down into the micromechanics of hair bundle deflection to answer the final question: exactly how do the hair bundle deflections occur for both BCV and ACS stimuli? This comes down to what happens at the interface between the receptor cilia and the otolithic membrane during stimulation.

At the striola the short, stiff hair bundles of the receptors project into holes in the otolithic membrane (49, 50, 63–65). So any wall motion of the holes in the column filament-gel layer structure of the otolithic membrane will produce endolymph fluid motion within the hole. In the striolar region, the hair cell bundles are only weakly attached at the top of the kinocilium (27), or not attached at all and are free standing (49). This fluid motion within the hole produces a drag force on the bundle, causing it to deflect. The fluid environment is so viscously dominated (Reynold's numbers—the ratio of inertial to viscous forces of 10^{-3} – 10^{-2}) that bundles move instantaneously with any fluid movement. In other words, this coupling of fluid motion to hair bundle is so strong that the hair bundle displacement follows the fluid displacement almost exactly. The viscous dominated environment results in bundle displacement matching fluid displacement almost exactly, so fluid displacement is synonymous with hair bundle displacement. This account would also apply to receptor activation by ACS, since the vibrometry shows that the utricular macula moves during high-frequency ACS as well as during BCV. In sum, we suggest that the actual stimulus causing hair bundle deflection is the fluid displacement around the cilia of the type I receptors (see **Box 1**).

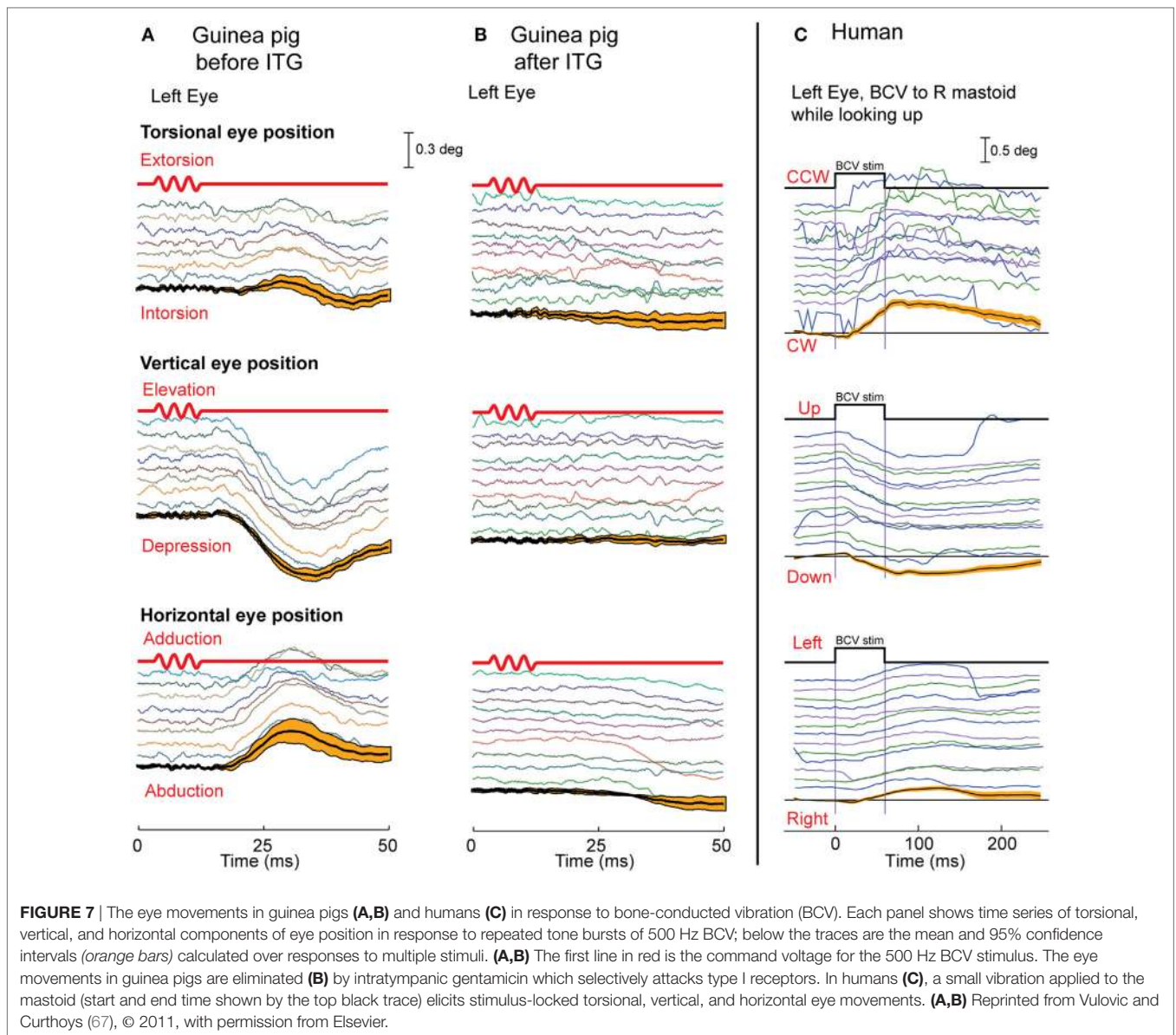
BOX 1 | Transduction model of Grant and Curthoys (62).

1. The otolithic system is underdamped. The transition from accelerometer mode to seismometer mode would not take place if the system were not underdamped.
2. The transition from accelerometer to seismometer takes place at the system undamped natural frequency (estimated to be around 600 Hz for humans).
3. In the accelerometer mode, head acceleration causes the otoconial layer (OL) to lag behind the neuroepithelial layer (NEL), producing a relative displacement between NEL and OL. This relative displacement deflects receptor hair bundles which activates the receptors.
4. In the seismometer mode at high frequencies, the OL remains at rest due to its inertia and the NEL is in motion, again producing relative displacement between the two layers and so again activating receptors.
5. Using vestibular-evoked myogenic potential (VEMP) test frequencies and acceleration magnitudes, we estimate the relative displacement between the two layers is around 50–80 nm. This displacement is small but sufficient to stimulate the short, stiff, loosely attached type I hair cell bundles in the striolar regions, while not large enough to activate extrastriolar type II hair bundles.
6. The model has implications for clinical testing: the ideal stimulus for otoliths and thus VEMPs is one with a very rapid rise time since the otolithic receptors are jerk detectors. That agrees with animal experimental (61) and clinical data (98) (see below) that short rise times are optimal for eliciting ocular vestibular-evoked myogenic potentials. Modeling of the neural data (62) indicates 750 Hz is probably the optimum frequency for testing VEMPs.

PHYSIOLOGY RELEVANT FOR CLINICAL TESTING

Suzuki et al. electrically stimulated the utricular nerve in cats and showed it caused eye movements with torsional, vertical, and horizontal components (66). We reasoned that if 500 Hz BCV is a specific otolithic stimulus, it should generate a similar pattern of eye movements to those reported by Suzuki et al., and Vulovic and Curthoys (67) showed that brief 500 Hz BCV pulses of the skull of an alert guinea pig generated eye movements with horizontal vertical and torsional components similar to those Suzuki et al. found (**Figure 7**). These eye movements are due to vestibular as opposed to cochlear activation, because after intratympanic injection of gentamicin to the guinea pig, a procedure which selectively kills vestibular type I receptor cells (68, 69), the BCV evoked eye movements disappear but the indicator of cochlear function, the ABR response, remains (67).

Do these conclusions apply to human otolith-induced eye movements? In some healthy subjects (without any symptoms of superior canal dehiscence) we used fast high resolution video recording to record eye movements, and found that brief bursts of 500 Hz BCV of one mastoid delivered by a small clinical bone oscillator (Radioear B-71) caused small but systematic and reliable stimulus-locked eye movement responses with horizontal, vertical, and torsional components (**Figure 7**) at a short latency of about 20 ms or less (70). In these experiments, the subjects were biting on a bite-bar during the BCV stimulation to minimize head rotation and so minimize semicircular canal stimulation. Prior to such eye movements there would be electromyographic (EMG) potentials in the ocular muscles to cause the eye movement



response, and it is these potentials in eye muscles which are recorded in VEMPs.

Air-conducted sound and BCV both activate both utricular and saccular afferents (29, 31, 33). Saccular afferents in guinea pigs do have a lower threshold to ACS than utricular afferents. But afferents from both maculae respond to both ACS and BCV (30, 31, 33). So how then is it possible to differentially assess utricular as opposed to saccular function? Curthoys put forward the original idea that the differential assessment of utricular and saccular function can come from the largely differential neural projections of these two systems (71). Physiology shows that short latency saccular projections to inferior oblique are weak, whereas saccular projections to neck and spinal motoneurons are strong (72). The work of Suzuki et al. (66) had shown that utricular projections

to inferior oblique are strong, so Curthoys suggested that measuring the contralateral oVEMP—from the inferior oblique eye muscles—largely reflects the activation of contralateral utricular afferents by either ACS or BCV. Saccular projection to ipsilateral neck motoneurons is strong, so it was suggested that measuring the ipsilateral cVEMP from stretched neck muscles shows largely ipsilateral saccular function (71) (Figure 8). In this way, VEMPs can provide tests of utricular and saccular function not because of stimuli which selectively activate one or other of the two maculae, but by measuring responses which are predominantly determined by the differential neural projection of utricular as opposed to saccular projections to various muscle groups (Figure 8). This suggestion caused considerable controversy at the time (73, 74); however, data from patients with partial unilateral vestibular

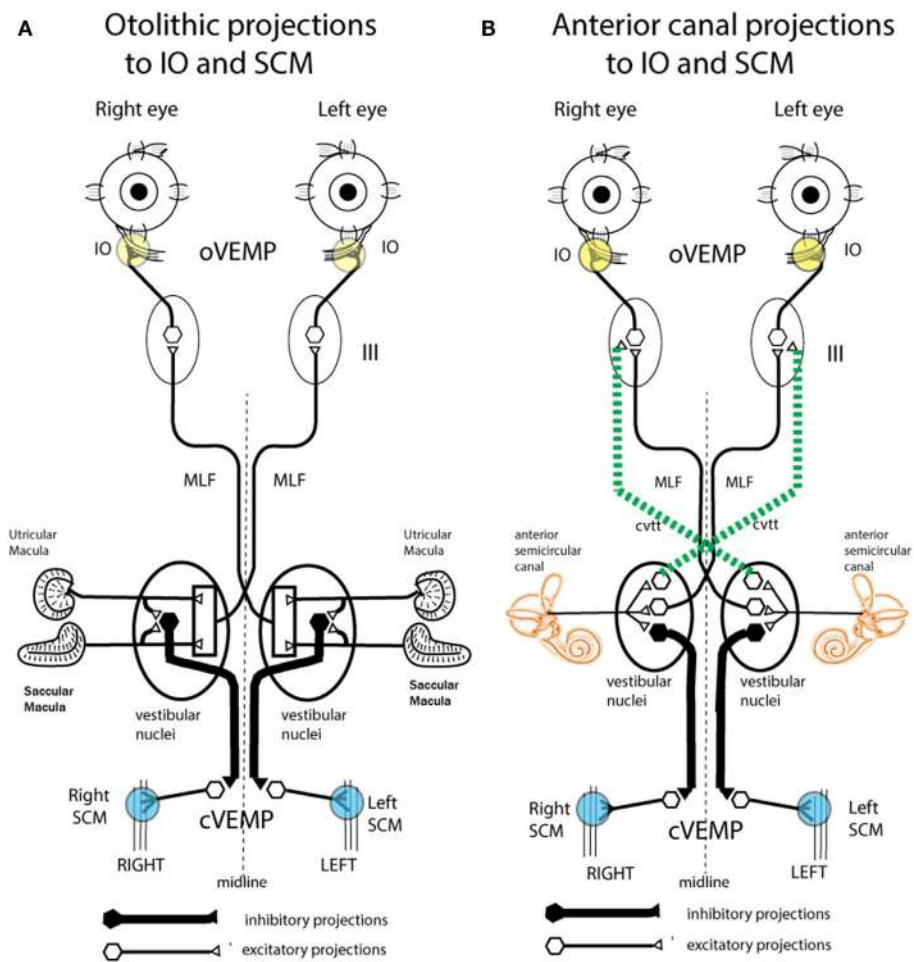


FIGURE 8 | Schematic representations of the major neural projections from vestibular receptors to the eye muscles and the neck muscles. **(A)** The otolithic projections to inferior oblique eye muscle (IO) and sternocleidomastoid muscle (SCM). **(B)** The analogous projections of the anterior semicircular canal neurons to the IO and SCM (72). Stimulation in animals with intact labyrinths causes the neural connections shown on the left panel to be activated. However, after a semicircular canal dehiscence (SCD), the anterior semicircular canals are also activated by sound and vibration, so the neural projections on the right come into play. The green dotted lines represent the projection from the anterior canal neurons in the vestibular nucleus to the contralateral third nerve nucleus *via* the crossed ventral-tegmental track. It appears that it is this combination of otolithic and canal afferent activation which in part results in the enhanced ocular vestibular-evoked myogenic potential (oVEMP) and cervical vestibular-evoked myogenic potential (cVEMP) responses after SCD. **(A)** Reprinted by permission from John Wiley and Sons, Curthoys et al. (80), © 2011. **(B)** Reprinted by permission from Springer Nature, Curthoys (81), © 2017.

neuritis have provided evidence confirming those suggestions. In response to ACS or BCV some patients show *selective* loss of the contralateral oVEMP n10, but preservation of the ipsilateral cVEMP p13–n23 (75, 76). Other patients show the converse: symmetrical oVEMPs but asymmetrical cVEMPs: the ipsilateral cVEMP is reduced or eliminated, yet the oVEMP is not detectably affected (77). The logical consequence of that dissociation is that the two responses, oVEMP and cVEMP, must be generated from different sense organs—because to the same stimulus one response is affected, the other is not. Since the utricular afferents travel in the superior nerve and project to contralateral inferior oblique, it is most likely the utricular afferents which are affected. In light of these results, the Curthoys (71, 74) suggestion is now accepted: “Ocular vestibular evoked potentials are mainly

dependent on utricular pathway function” [(78), p. 1843] and “The oVEMP originates predominantly from utricular afferents” [(79), p. 1051].

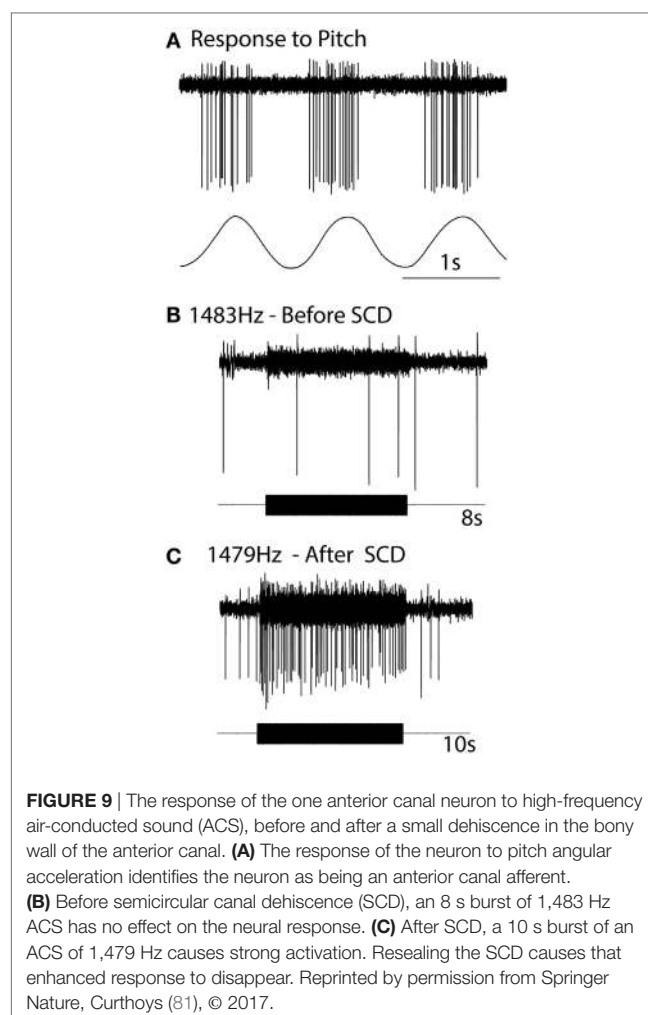
The stimulus frequency usually used for clinical testing of VEMPs is 500 Hz, and that frequency causes fairly selective activation of otolithic irregular neurons: at 500 Hz semicircular canal afferents with irregular resting discharge are not usually activated by sound or vibration in animals with normally encased bony labyrinths, at least up to BCV stimulus levels of 2 g or 130 dB SPL ACS (28, 31). Carey et al. reported that to elicit phase locking in irregular canal afferents in the chinchilla with a normally encased labyrinth required an extremely high intensity (135 dB SPL) (82). We have confirmed that result in guinea pigs (81, 83). Regular canal and otolith afferents are not

activated usually by physiological levels of ACS and BCV. Higher level stimuli may cause them to be activated, but such levels are not clinically realistic. So usually there is little or no contribution from regular or irregular semicircular canal afferents during VEMP testing. That is changed in patients with a thinning—a dehiscence or window (fenestra or SCD) of the bony wall of the semicircular canal, who show very large VEMP potentials (discussed below).

The physiological results show that an SCD changes the neural response. After making an opening into the bony wall of the anterior canal, the procedure resulted in phase-locked activation of irregular canal afferents at a much lower intensity (96 dB SPL) than with the labyrinth encased (135 dB SPL) (82). These SCD-enhanced vestibular neural responses are consistent with the results from patients with a CT-verified SCD who show enhanced VEMPs to sound and vibration and nystagmus in the plane of the dehiscent canal during maintained tonal stimulation (84). However, it should be emphasized that both the neural and clinical results are variable; not all patients with CT-verified SCD develop the same classic symptoms, and there is considerable variability in the neural results (85). This is not surprising since the fenestra varies from patient to patient in humans and animals, and many other factors have the potential for influencing the results, such as collapse of the membranous duct (86).

The definitive evidence about the neural response in SCD comes from the response of individual neurons where the same neuron was recorded both before and after the SCD and in some cases after resealing the SCD (Figure 9). After SCD, guinea pig irregular semicircular canal afferents, previously unresponsive to ACS or BCV in animals with fully encased labyrinths, respond vigorously with low threshold to the same stimulus magnitude which was ineffective before SCD (83, 87). Maintained sound or vibration results in a maintained high firing rate in irregular anterior canal neurons. This has been confirmed by Iversen et al. (88), who also confirmed the report by Curthoys and Grant (53) that an SCD causes a slow change in firing of regular canal afferents to maintained sound. This change in neural firing corresponds to the cupula deflection caused by endolymph movement due to the SCD causing an impedance pumping type of action. Such a high firing rate would cause a maintained nystagmus in human patients (the Tullio phenomenon) (81). Nystagmus caused by such phase-locked activation in human patients would be expected to have abrupt onset and offset, as in fact happens in some patients in the clinical test called vibration-induced nystagmus (89).

Why should an SCD cause semicircular canal neurons previously unaffected by ACS or BCV now to respond to ACS and BCV? The SCD is a third window and so ACS and BCV cause larger fluid displacement in the duct (90, 91), and irregular canal afferents synapsing on type I receptors at the crest of the crista (43, 92, 93) are activated by these fluid displacements (83). Although similar structurally and physiologically to otolith type I receptors, canal type I receptors are not usually activated by ACS or BCV, because the sealed bony wall of the canal limits the amplitude of the sound-induced or



vibration-induced fluid displacement in the canal. We reasoned that after an SCD, the increased fluid displacement is sufficient to deflect the short stiff cilia of type I semicircular canal receptors on the crista, and so irregular canal afferents would show phase-locked activation after SCD to both ACS and BCV, and in humans, canal neurons would thus contribute to the VEMP response as was found (83).

Such an outcome in human SCD patients would result in lower VEMP thresholds, as is observed. In addition, irregular anterior canal neurons project to contralateral inferior oblique, and so after SCD these neurons would now contribute to and enhance the oVEMP n10 response in the contralateral inferior oblique after SCD (Figure 10). Also by virtue of their ipsilateral (inhibitory) projection to SCM (72) (Figure 8), the activity of these canal afferents would enhance the cVEMP over the ipsilateral SCM.

In summary, the physiological evidence predicts the enhanced VEMP response seen after SCD. Patients with CT-verified SCD show VEMPs in response to very high-frequency stimulation which is ineffective in healthy subjects with intact bony

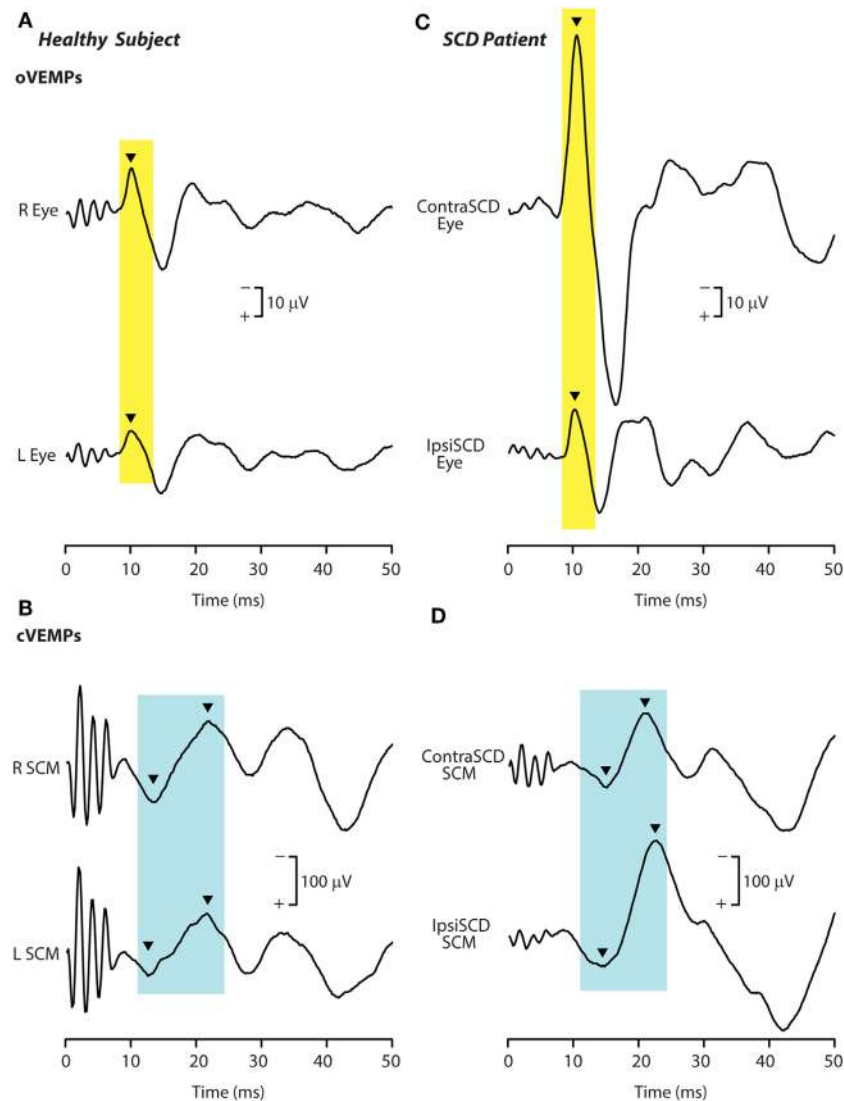


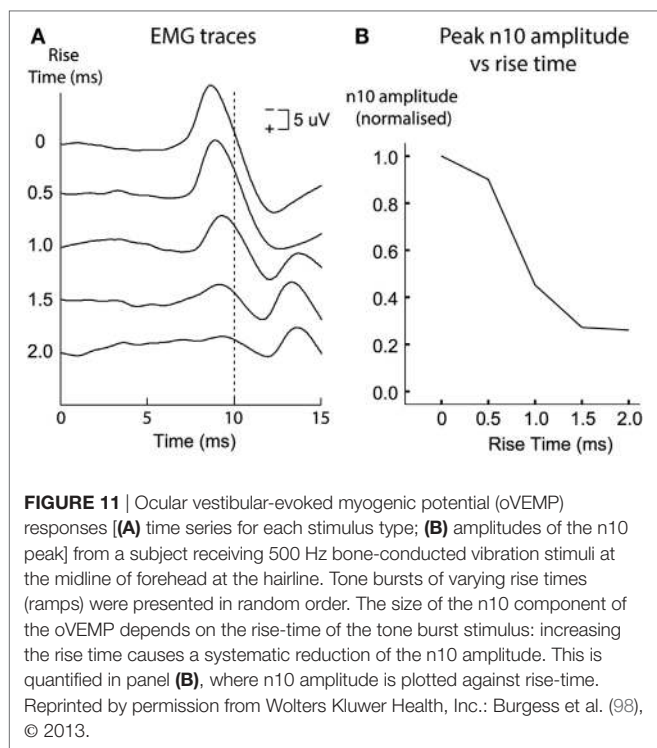
FIGURE 10 | Recordings of ocular vestibular-evoked myogenic potentials (oVEMPs) (A,C) and cervical vestibular-evoked myogenic potentials (cVEMPs) (B,D) to 500 Hz bone-conducted vibration (BCV) from a healthy subject (A,B) and a patient with semicircular canal dehiscence (SCD) (C,D). In each record, the stimulus onset occurred at time 0. In the healthy subject, BCV at the midline of forehead at the hairline (Fz) causes symmetric oVEMP beneath both eyes, with approximately equal amplitude oVEMP n10 components (arrowheads). By contrast, the same Fz stimulus causes an asymmetric n10 component of the oVEMP response in the patient: the oVEMP n10 recorded from beneath the contralesional eye is much larger than the oVEMP n10 recorded from beneath the ipsilesional eye, and is also much larger than seen in the healthy subject. In response to BCV at Fz, both subjects show clear cVEMP p13–n23 [arrowheads in (B,D)]. The response in the ipsilesional sternocleidomastoid muscle (SCM) in the patient is larger than in the patient's contralesional SCM, but the asymmetry is not as great as in the same patient's oVEMP traces. The cVEMP responses of the normal subject are more symmetrical than in the SCD patient. Reprinted by permission from Wolters Kluwer Health, Inc.: Manzari et al. (94), © 2012.

labyrinth (95): a single VEMP test using 4,000 or 8,000 Hz elicits clear oVEMPs in such patients. Patients may have trouble even hearing the 8,000 Hz stimulus, which produces clear oVEMP n10 (95).

Afferents from other canals would probably not be affected by the SCD in one canal because after SCD the enhanced fluid displacement is apparently mainly directed to the canal with the new “third window.” This is in accord with what is usually found with human patients—the nystagmus produced by

sound usually aligns with the canal in which the fenestra is located (96).

So how is an oVEMP n10 in human subjects to ACS or BCV normally caused? Probably the most effective otolithic stimulus is a light tap with a tendon hammer to the skull at the midline of forehead at the hairline, because that is a high-jerk stimulus (97), and that pulse of jerk would be expected to cause simultaneous activation in many otolithic irregular afferents. We know it is the very onset of the stimulus which is effective in generating human



oVEMP n10. Using very short rise-times (ramps) increases the magnitude of the oVEMP n10 (98) (Figure 11). Also, if a long duration 500 Hz stimulus is used and then its duration progressively reduced, the size of the oVEMP n10 for a stimulus duration of 2 ms is about the same as for a stimulus lasting 10 ms (99). The paradoxical aspect is that such a short stimulus sounds (and feels) pathetically weak, but the EMG measures show it is just as effective at eliciting an oVEMP n10 response as a long duration 10 ms stimulus (99) which subjectively appears to be a much stronger stimulus. Both results point to the very onset of the stimulus as being of great importance in determining the size of the oVEMP n10.

The widespread use of these tests together with the use of the video head impulse test of the function of all the semicircular canals has refined vestibular diagnosis of peripheral vestibular disorders. It is now clear that some patients have normal semicircular canal function bilaterally but total loss of otolith function unilaterally—as shown by reduced or absent oVEMP and cVEMP from one labyrinth. Even with unilateral loss of just the utricular macula with completely normal canal function and normal saccular function (100). These selective deficits support the contention that any individual sense organ of the vestibular labyrinth can exhibit dysfunction while the remainder of the labyrinth functions normally.

There is strong physiological evidence underpinning the initial step of VEMP—the activation of vestibular receptors by sound or vibration. The extensive projection of vestibular nuclei allow for many VEMP to be recorded. These with very short latency (cVEMPs and oVEMPs) have been favored for clinical evaluation of otolith function (see Box 2 for summary).

BOX 2 | Summary.

- There are two kinds of otolithic receptor hair cells—amphora-shaped type I receptors and barrel-shaped type II receptors—and they are intermingled across the utricular and saccular maculae. There is a special band of receptors called the striola, on both the utricular macula and the saccular macula, where there is an increased concentration of receptors with short stiff cilia and poor attachment to the overlying otolithic membrane.
- Afferent neurons from the striolae form calyx synapses on type I receptors and have irregular resting discharge. It is these afferents which are activated by both sound and vibration. In animals with normally encased bony labyrinths, neurons with regular resting discharge are not activated by ACS or bone-conducted vibration (BCV) up to the maximum levels which were used.
- Bone-conducted vibration is a much more effective and reliable stimulus—vestibular neural thresholds to BCV are around the level for auditory brainstem response (ABR) threshold, whereas vestibular neural thresholds for ACS are around 70 dB above ABR threshold.
- The action potentials in the irregular afferents activated by sound and vibration are phase-locked to a particular band of phase angles of the stimulus waveform, up to frequencies well above 1,000 Hz for both ACS and BCV. In order to elicit this tight phase locking, each cycle of the waveform is the effective stimulus—each cycle is deflecting the hair bundles of the receptors.
- Grant and Curthoys (62) have suggested that the utricular macula operates both as an accelerometer at low frequencies and as a seismometer at high frequencies. On this model, at low frequencies the otoconia move relative to the receptor cell body (accelerometer mode), but at high frequencies the otoconia are stationary and the receptors move relative to the otoconia (seismometer mode).
- In both cases, the hair bundles are deflected relative to the cell body, so the receptors are activated both at low (accelerometer) and at high (seismometer) frequencies. That is confirmed by recording of the field potential of the utricular receptor hair cells—the utricular microphonic—which shows that utricular receptors are activated by the BCV stimulus up to high frequencies. It is stressed that the vestibular microphonic occurs without any input from the cochlea.
- Direct measures of utricular macula movement show that the macula moves up and down during vibration stimulation (and sound) up to frequencies of thousands of Hertz. The movements are very small, but *in vitro* studies (52) have shown that individual vestibular receptors have thresholds of nanometers of displacement, similar to the thresholds of cochlear receptors.
- In this way, 500 Hz mastoid vibration activates otolithic receptors and results in eye movements with horizontal, vertical, and torsional components, in human subjects consistent with utricular nerve activation at such high frequencies.
- Surface electrodes over muscle groups can record the electromyographic potentials evoked by abrupt stimulation by ACS and BCV, and thus these vestibular evoked myogenic potentials (VEMPs) are being used in the clinic to indicate otolith function.
- Because of the largely differential projection of the utricular macula to eye muscles and of the saccular macula to neck muscles, it has been possible to index predominantly utricular function by measuring the ocular vestibular-evoked myogenic potential by surface electrodes beneath the eyes as the subject looks up. Surface electrodes over tensed neck muscles record the cervical vestibular-evoked myogenic potential which indexes predominantly saccular function.

AUTHOR CONTRIBUTIONS

IC wrote the paper. JG wrote the section about the accelerometer–seismometer model. AB contributed to the section about clinical evidence. CP and DB contributed to the section about vestibular microphonics and vibrometry. LM contributed to the section about clinical evidence. All authors reviewed the text of the final paper.

ACKNOWLEDGMENTS

Much of the work reported here has been supported by the Garnett Passe and Rodney Williams Memorial Foundation, and we are very grateful for their continued support, and also for the support of the National Health and Medical Research Council of Australia.

REFERENCES

- Weber KP, Rosengren SM. Clinical utility of ocular vestibular-evoked myogenic potentials (oVEMPs). *Curr Neurol Neurosci Rep* (2015) 15:22. doi:10.1007/s11910-015-0548-y
- Dlugaiczek J. Ocular vestibular evoked myogenic potentials: where are we now? *Otol Neurotol* (2017) 38:E513–21. doi:10.1097/MAO.0000000000001478
- Clark B, Graybiel A. Perception of the postural vertical in normals and subjects with labyrinthine defects. *J Exp Psychol* (1963) 65:490–4. doi:10.1037/h0045606
- Diamond SG, Markham CH, Furuya N. Binocular counter-rolling during sustained body tilt in normal humans and in a patient with unilateral vestibular nerve-section. *Ann Otol Rhinol Laryngol* (1982) 91:225–9. doi:10.1177/000348948209100222
- Graybiel A. Oculogravic illusion. *AMA Arch Ophthalmol* (1952) 48:605–15. doi:10.1001/archoph.1952.00920010616007
- Lichtenberg BK, Young LR, Arrott AP. Human ocular counter-rolling induced by varying linear accelerations. *Exp Brain Res* (1982) 48:127–36. doi:10.1007/BF00239580
- Miller EF, Fregly AR, Graybiel A. Visual horizontal-perception in relation to otolith-function. *Am J Psychol* (1968) 81:488–96. doi:10.2307/1421053
- Schone H. On the role of gravity in human spatial orientation. *Aerosp Med* (1964) 35:764–72.
- Rudisill HE, Hain TC. Lower extremity myogenic potentials evoked by acoustic stimuli in healthy adults. *Otol Neurotol* (2008) 29:688–92. doi:10.1097/MAO.0b013e3181730377
- Cherchi M, Bellinaso NP, Card K, Covington A, Krumpke A, Pfeifer MS, et al. Sound evoked triceps myogenic potentials. *Otol Neurotol* (2009) 30:545–50. doi:10.1097/MAO.0b013e31819d89eb
- Colebatch JG, Halmagyi GM, Skuse NF. Myogenic potentials generated by a click-evoked vestibulocollic reflex. *J Neurol Neurosurg Psychiatry* (1994) 57:190–7. doi:10.1136/jnnp.57.2.190
- Rosengren SM, Todd NPM, Colebatch JG. Vestibular-evoked extraocular potentials produced by stimulation with bone-conducted sound. *Clin Neurophysiol* (2005) 116:1938–48. doi:10.1016/j.clinph.2005.03.019
- Iwasaki S, McGarvie LA, Halmagyi GM, Burgess AM, Kim J, Colebatch JG, et al. Head taps evoke a crossed vestibulo-ocular reflex. *Neurology* (2007) 68:1227–9. doi:10.1212/01.wnl.0000259064.80564.21
- Todd NP, Rosengren SM, Aw ST, Colebatch JG. Ocular vestibular evoked myogenic potentials (OVEMPs) produced by air- and bone-conducted sound. *Clin Neurophysiol* (2007) 118:381–90. doi:10.1016/j.clinph.2006.09.025
- Halmagyi GM, Yavor RA, Colebatch JG. Tapping the head activates the vestibular system: a new use for the clinical reflex hammer. *Neurology* (1995) 45:1927–9. doi:10.1212/WNL.45.10.1927
- Iwasaki S, Chihara Y, Smulders YE, Burgess AM, Halmagyi GM, Curthoys IS, et al. The role of the superior vestibular nerve in generating ocular vestibular-evoked myogenic potentials to bone conducted vibration at Fz. *Clin Neurophysiol* (2009) 120:588–93. doi:10.1016/j.clinph.2008.12.036
- Colebatch JG, Halmagyi GM. Vestibular evoked potentials in human neck muscles before and after unilateral vestibular deafferentation. *Neurology* (1992) 42:1635–6. doi:10.1212/WNL.42.8.1635
- Maqsood A, Anis-ur-Rehman M, Gul IH. Chemical composition, density, specific gravity, apparent porosity, and thermal transport properties of volcanic rocks in the temperature range 253 to 333 K. *J Chem Eng Data* (2003) 48:1310–4. doi:10.1021/je034077p
- Lopez I, Ishiyama G, Tang Y, Frank M, Baloh RW, Ishiyama A. Estimation of the number of nerve fibers in the human vestibular endorgans using unbiased stereology and immunohistochemistry. *J Neurosci Methods* (2005) 145:37–46. doi:10.1016/j.jneumeth.2004.11.024

FUNDING

IC receives funding from a Conjoint Grant from the Garnett Passe and Rodney Williams Memorial Foundation: this grant funds the salary of AB. DB is in receipt of a Senior Research Fellowship from the Garnett Passe and Rodney Williams Memorial Foundation.

- Bergström B. Morphology of the vestibular nerve. III. Analysis of the calibers of the myelinated vestibular nerve fibers in man at various ages. *Acta Otolaryngol* (1973) 76:331–8. doi:10.3109/00016487309121518
- Baloh RW, Honrubia V. *Clinical Neurophysiology of the Vestibular System*. 2nd ed. Philadelphia, PA: F. A. Davis (1990).
- DeVries H. The mechanics of the labyrinth otoliths. *Acta Otolaryngol* (1950) 38:262–73. doi:10.3109/00016485009118384
- Grant W, Best W. Otolith-organ mechanics – lumped parameter model and dynamic-response. *Aviat Space Environ Med* (1987) 58:970–6.
- Cotton JR, Grant JW. A finite element method for mechanical response of hair cell ciliary bundles. *J Biomech Eng* (2000) 122:44–50. doi:10.1115/1.429626
- Dunlap MD, Grant JW. Experimental measurement of utricle system dynamic response to inertial stimulus. *J Assoc Res Otolaryngol* (2014) 15:511–28. doi:10.1007/s10162-014-0456-x
- Grant JW, Best WA, Lonigro R. Governing equations of motion for the otolith organs and their response to a step change in velocity of the skull. *J Biomech Eng* (1984) 106:302–8. doi:10.1115/1.3138498
- Lindeman HH. Studies on the morphology of the sensory regions of the vestibular apparatus with 45 figures. *Ergeb Anat Entwicklungsgesch* (1969) 42:1–113.
- Curthoys IS, Kim J, McPhedran SK, Camp AJ. Bone conducted vibration selectively activates irregular primary otolithic vestibular neurons in the guinea pig. *Exp Brain Res* (2006) 175:256–67. doi:10.1007/s00221-006-0544-1
- Curthoys IS, Vulovic V. Vestibular primary afferent responses to sound and vibration in the guinea pig. *Exp Brain Res* (2011) 210:347–52. doi:10.1007/s00221-010-2499-5
- Curthoys IS, Vulovic V, Burgess AM, Manzari L, Sokolic L, Pogson J, et al. Neural basis of new clinical vestibular tests: otolithic neural responses to sound and vibration. *Clin Exp Pharmacol Physiol* (2014) 41:371–80. doi:10.1111/1440-1681.12222
- Curthoys IS, Vulovic V, Burgess AM, Sokolic L, Goonetilleke SC. The response of guinea pig primary utricular and saccular irregular neurons to bone-conducted vibration (BCV) and air-conducted sound (ACS). *Hear Res* (2016) 331:131–43. doi:10.1016/j.heares.2015.10.019
- Curthoys IS, Vulovic V, Pogson J, Sokolic L. Responses of guinea pig primary vestibular afferents to low frequency (50–100 Hz) bone conducted vibration (BCV) – the neural basis of vibration induced nystagmus. *Program No 57406 2012 Neuroscience Meeting Planner [Online]*. New Orleans, LA: Society for Neuroscience (2013).
- Curthoys IS, Vulovic V, Sokolic L, Pogson J, Burgess AM. Irregular primary otolith afferents from the guinea pig utricular and saccular maculae respond to both bone conducted vibration and to air conducted sound. *Brain Res Bull* (2012) 89:16–21. doi:10.1016/j.brainresbull.2012.07.007
- Fernandez C, Goldberg JM. Physiology of peripheral neurons innervating otolith organs of the squirrel monkey. I. Response to static tilts and to long-duration centrifugal force. *J Neurophysiol* (1976) 39:970–84. doi:10.1152/jn.1976.39.5.970
- McCue MP, Guinan JJ Jr. Acoustically responsive fibers in the vestibular nerve of the cat. *J Neurosci* (1994) 14:6058–70. doi:10.1523/JNEUROSCI.14-10-06058.1994
- McCue MP, Guinan JJ Jr. Sound-evoked activity in primary afferent neurons of a mammalian vestibular system. *Am J Otol* (1997) 18:355–60.
- Murofushi T, Curthoys IS, Topple AN, Colebatch JG, Halmagyi GM. Responses of guinea pig primary vestibular neurons to clicks. *Exp Brain Res* (1995) 103:174–8. doi:10.1007/BF00241975
- Young ED, Fernandez C, Goldberg JM. Responses of squirrel monkey vestibular neurons to audio-frequency sound and head vibration. *Acta Otolaryngol* (1977) 84:352–60. doi:10.3109/00016487709123977

39. Zhu H, Tang X, Wei W, Maklad A, Mustain W, Rabbitt R, et al. Input-output functions of vestibular afferent responses to air-conducted clicks in rats. *J Assoc Res Otolaryngol* (2014) 15:73–86. doi:10.1007/s10162-013-0428-6
40. Zhu H, Tang X, Wei W, Mustain W, Xu Y, Zhou W. Click-evoked responses in vestibular afferents in rats. *J Neurophysiol* (2011) 106:754–63. doi:10.1152/jn.00003.2011
41. Curthoys IS, MacDougall HG, Vidal PP, de Waele C. Sustained and transient vestibular systems: a physiological basis for interpreting vestibular function. *Front Neurol* (2017) 8:117. doi:10.3389/fneur.2017.00117
42. Uzun-Coruhlu H, Curthoys IS, Jones AS. Attachment of the utricular and saccular maculae to the temporal bone. *Hear Res* (2007) 233:77–85. doi:10.1016/j.heares.2007.07.008
43. Desai SS, Zeh C, Lysakowski A. Comparative morphology of rodent vestibular periphery. I. Saccular and utricular maculae. *J Neurophysiol* (2005) 93:251–66. doi:10.1152/jn.00746.2003
44. Watanuki K, Schuknecht HF. A morphological study of human vestibular sensory epithelia. *Arch Otolaryngol* (1976) 102:583–8. doi:10.1001/archotol.1976.00780150051001
45. Spoon C, Grant W. Biomechanics of hair cell kinocilia: experimental measurement of kinocilium shaft stiffness and base rotational stiffness with Euler-Bernoulli and Timoshenko beam analysis. *J Exp Biol* (2011) 214:862–70. doi:10.1242/jeb.051151
46. Watanuki K, Meyer zum Gottesberge A. Morphological observations of the sensory epithelium of the macula sacculi and utriculi in the guinea pig. *Arch Klin Exp Ohren Nasen Kehlkopfheilkd* (1971) 200:136–44. doi:10.1007/BF00418197
47. Fernandez C, Goldberg JM, Baird RA. The vestibular nerve of the chinchilla. III. Peripheral innervation patterns in the utricular macula. *J Neurophysiol* (1990) 63:767–80. doi:10.1152/jn.1990.63.4.767
48. Goldberg JM, Desmadryl G, Baird RA, Fernandez C. The vestibular nerve of the chinchilla. IV. Discharge properties of utricular afferents. *J Neurophysiol* (1990) 63:781–90. doi:10.1152/jn.1990.63.4.781
49. Lim DJ. Morphological and physiological correlates in cochlear and vestibular sensory epithelia. *Scan Electron Microsc* (1976) 2:269–76.
50. Lim DJ. Fine morphology of the otoconial membrane and its relationship to the sensory epithelium. *Scan Electron Microsc* (1979) 3:929–38.
51. Songer JE, Eatock RA. Tuning and timing in mammalian type I hair cells and calyceal synapses. *J Neurosci* (2013) 33:3706–24. doi:10.1523/JNEUROSCI.4067-12.2013
52. Geleoc GSG, Lennan GWT, Richardson GP, Kros CJ. A quantitative comparison of mechano-electrical transduction in vestibular and auditory hair cells of neonatal mice. *Proc Biol Sci* (1997) 264:611–21. doi:10.1098/rspb.1997.0087
53. Curthoys IS, Grant JW. In what way is an air conducted sound an otolithic stimulus? PS-927. *Abstr Assoc Res Otolaryngol* (2016) 39:568.
54. Palmer AR, Russell IJ. Phase-locking in the cochlear nerve of the guinea-pig and its relation to the receptor potential of inner hair-cells. *Hear Res* (1986) 24:1–15. doi:10.1016/0378-5955(86)90002-X
55. Rose JE, Brugge JF, Anderson DJ, Hind JE. Phase-locked response to low-frequency tones in single auditory nerve fibers of the squirrel monkey. *J Neurophysiol* (1967) 30:769–93. doi:10.1152/jn.1967.30.4.769
56. Fettiplace R. Hair cell transduction, tuning, and synaptic transmission in the mammalian cochlea. *Compr Physiol* (2017) 7:1197–227. doi:10.1002/cphy.c160049
57. Pastras CJ, Curthoys IS, Brown DJ. In vivo recording of the vestibular microphonic in mammals. *Hear Res* (2017) 354:38–47. doi:10.1016/j.heares.2017.07.015
58. Brown DJ, Pastras CJ, Curthoys IS. Electrophysiological measurements of peripheral vestibular function – a review of electrovestibulography. *Front Syst Neurosci* (2017) 11:34. doi:10.3389/fnsys.2017.00034
59. Pastras C, Curthoys IS, Brown D. Dynamic response and sensitivity of the utricular macula, measured in vivo using laser Doppler vibrometry in guinea pigs. PS547. *Abstr Assoc Res Otolaryngol* (2018) 41:342.
60. Tullio P. *L'orecchio*. Bologna: L. Capelli Editore (1928).
61. Jones TA, Jones SM, Vijayakumar S, Brugeaud A, Bothwell M, Chabbert C. The adequate stimulus for mammalian linear vestibular evoked potentials (VsEPs). *Hear Res* (2011) 280:133–40. doi:10.1016/j.heares.2011.05.005
62. Grant W, Curthoys I. Otoliths – accelerometer and seismometer; implications in vestibular evoked myogenic potential (VEMP). *Hear Res* (2017) 353:26–35. doi:10.1016/j.heares.2017.07.012
63. Lim DJ. Vestibular sensory organs – scanning electron microscopic investigation. *Arch Otolaryngol* (1971) 94:69–76. doi:10.1001/archotol.1971.00770070105013
64. Lim DJ, Anniko M. Developmental morphology of the mouse inner ear. A scanning electron microscopic observation. *Acta Otolaryngol Suppl* (1985) 422:1–69. doi:10.3109/00016488509121766
65. Lim DJ, Lane WC. Vestibular sensory epithelia – a scanning electron microscopic observation. *Arch Otolaryngol* (1969) 90:283–92. doi:10.1001/archotol.1969.00770030285007
66. Suzuki JI, Tokumasu K, Goto K. Eye movements from single utricular nerve stimulation in the cat. *Acta Otolaryngol* (1969) 68:350–62. doi:10.3109/00016486909121573
67. Vulovic V, Curthoys IS. Bone conducted vibration activates the vestibulo-ocular reflex in the guinea pig. *Brain Res Bull* (2011) 86:74–81. doi:10.1016/j.brainresbull.2011.06.013
68. Lyford-Pike S, Vogelheim C, Chu E, Della Santina CC, Carey JP. Gentamicin is primarily localized in vestibular type I hair cells after intratympanic administration. *J Assoc Res Otolaryngol* (2007) 8:497–508. doi:10.1007/s10162-007-0093-8
69. Lue J-H, Day A-S, Cheng P-W, Young Y-H. Vestibular evoked myogenic potentials are heavily dependent on type I hair cell activity of the saccular macula in guinea pigs. *Audiol Neurootol* (2009) 14:59–66. doi:10.1159/000156701
70. Cornell ED, Burgess AM, MacDougall HG, Curthoys IS. Bone conducted vibration to the mastoid produces horizontal, vertical and torsional eye movements. *J Vestib Res* (2015) 25:91–6. doi:10.3233/VES-150550
71. Curthoys IS. A critical review of the neurophysiological evidence underlying clinical vestibular testing using sound, vibration and galvanic stimuli. *Clin Neurophysiol* (2010) 121:132–44. doi:10.1016/j.clinph.2009.09.027
72. Uchino Y, Kushiro K. Differences between otolith- and semicircular canal-activated neural circuitry in the vestibular system. *Neurosci Res* (2011) 71:315–27. doi:10.1016/j.neures.2011.09.001
73. Colebatch JG. Sound conclusions? *Clin Neurophysiol* (2010) 121:124–6. doi:10.1016/j.clinph.2009.09.026
74. Curthoys IS. A balanced view of the evidence leads to sound conclusions. A reply to J.G. Colebatch “Sound conclusions?” *Clin Neurophysiol* (2010) 121:977–8. doi:10.1016/j.clinph.2010.01.025
75. Manzari L, Tedesco A, Burgess AM, Curthoys IS. Ocular vestibular-evoked myogenic potentials to bone-conducted vibration in superior vestibular neuritis show utricular function. *Otolaryngol Head Neck Surg* (2010) 143:274–80. doi:10.1016/j.otohns.2010.03.020
76. Curthoys IS, Iwasaki S, Chihara Y, Ushio M, McGarvie LA, Burgess AM. The ocular vestibular-evoked myogenic potential to air-conducted sound; probable superior vestibular nerve origin. *Clin Neurophysiol* (2011) 122:611–6. doi:10.1016/j.clinph.2010.07.018
77. Manzari L, Burgess AM, Curthoys IS. Ocular and cervical vestibular evoked myogenic potentials in response to bone-conducted vibration in patients with probable inferior vestibular neuritis. *J Laryngol Otol* (2012) 126:683–91. doi:10.1017/S0022215112000692
78. Papathanasiou ES. The evidence is finally here: ocular vestibular evoked myogenic potentials are mainly dependent on utricular pathway function. *Clin Neurophysiol* (2015) 126:1843–4. doi:10.1016/j.clinph.2015.01.007
79. Govender S, Colebatch JG. Location and phase effects for ocular and cervical vestibular-evoked myogenic potentials evoked by bone-conducted stimuli at midline skull sites. *J Neurophysiol* (2018) 119:1045–56. doi:10.1152/jn.00695.2017
80. Curthoys IS, Vulovic V, Burgess AM, Cornell ED, Mezey LE, MacDougall HG, et al. The basis for using bone-conducted vibration or air-conducted sound to test otolithic function. *Ann N Y Acad Sci* (2011) 1233:231–41. doi:10.1111/j.1749-6632.2011.06147.x
81. Curthoys IS. The new vestibular stimuli: sound and vibration-anatomical, physiological and clinical evidence. *Exp Brain Res* (2017) 235:957–72. doi:10.1007/s00221-017-4874-y
82. Carey JP, Hirvonen TP, Hullar TE, Minor LB. Acoustic responses of vestibular afferents in a model of superior canal dehiscence. *Otol Neurotol* (2004) 25:345–52. doi:10.1097/00129492-200405000-00024
83. Curthoys IS, Grant JW. How does high-frequency sound or vibration activate vestibular receptors? *Exp Brain Res* (2015) 233:691–9. doi:10.1007/s00221-014-4192-6

84. Cremer PD, Minor LB, Carey JP, Della Santina CC. Eye movements in patients with superior canal dehiscence syndrome align with the abnormal canal. *Neurology* (2000) 55:1833–41. doi:10.1212/WNL.55.12.1833
85. Ward BK, Carey JP, Minor LB. Superior canal dehiscence syndrome: lessons from the first 20 years. *Front Neurol* (2017) 8:177. doi:10.3389/fneur.2017.00177
86. Manzari L, Burgess AM, MacDougall HG, Curthoys IS. Enhanced otolith function in semicircular canal dehiscence. *Acta Otolaryngol* (2011) 131:107–12. doi:10.3109/00016489.2010.507780
87. Długańczyk J, Burgess AM, Goonetilleke S, Sokolic L, Curthoys IS. Superior canal dehiscence syndrome: relating clinical findings with vestibular neural responses from a guinea pig model. *Otol Neurotol* (2018) (in press).
88. Iversen M, Zhu H, Zhou W, Della Santina CC, Carey J, Rabbitt RD. The biophysical origins of Tullio phenomenon. PS546. *Abstr Assoc Res Otolaryngol* (2018) 41:341–2.
89. Dumas G, Curthoys IS, Lion A, Perrin P, Schmerber S. The skull vibration-induced nystagmus test of vestibular function – a review. *Front Neurol* (2017) 8:41. doi:10.3389/fneur.2017.00041
90. Chien W, Rosowski JJ, Ravicz ME, Rauch SD, Smullen J, Merchant SN. Measurements of stapes velocity in live human ears. *Hear Res* (2009) 249:54–61. doi:10.1016/j.heares.2008.11.011
91. Rosowski JJ, Songer JE, Nakajima HH, Brinsko KM, Merchant SN. Clinical, experimental, and theoretical investigations of the effect of superior semicircular canal dehiscence on hearing mechanisms. *Otol Neurotol* (2004) 25:323–32. doi:10.1097/00129492-200405000-00021
92. Desai SS, Ali H, Lysakowski A. Comparative morphology of rodent vestibular periphery. II. Cristae ampullares. *J Neurophysiol* (2005) 93:267–80. doi:10.1152/jn.00747.2003
93. Lysakowski A, Goldberg JM. A regional ultrastructural analysis of the cellular and synaptic architecture in the chinchilla cristae ampullares. *J Comp Neurol* (1997) 389:419–43. doi:10.1002/(SICI)1096-9861(19971222)389:3<419::AID-CNE5>3.0.CO;2-3
94. Manzari L, Burgess AM, McGarvie LA, Curthoys IS. Ocular and cervical vestibular evoked myogenic potentials to 500 Hz Fz bone-conducted vibration in superior semicircular canal dehiscence. *Ear Hear* (2012) 33:508–20. doi:10.1097/AUD.0b013e3182498c09
95. Manzari L, Burgess AM, McGarvie LA, Curthoys IS. An indicator of probable semicircular canal dehiscence: ocular vestibular evoked myogenic potentials to high frequencies. *Otolaryngol Head Neck Surg* (2013) 149:142–5. doi:10.1177/0194599813489494
96. Cremer PD, Migliaccio AA, Pohl DV, Curthoys IS, Davies L, Yavor RA, et al. Posterior semicircular canal nystagmus is conjugate and its axis is parallel to that of the canal. *Neurology* (2000) 54:2016–20. doi:10.1212/WNL.54.10.2016
97. Iwasaki S, Smulders YE, Burgess AM, McGarvie LA, MacDougall HG, Halmagyi GM, et al. Ocular vestibular evoked myogenic potentials to bone conducted vibration of the midline forehead at Fz in healthy subjects. *Clin Neurophysiol* (2008) 119:2135–47. doi:10.1016/j.clinph.2008.05.028
98. Burgess AM, Mezey LE, Manzari L, MacDougall HG, McGarvie LA, Curthoys IS. Effect of stimulus rise-time on the ocular vestibular-evoked myogenic potential to bone-conducted vibration. *Ear Hear* (2013) 34:799–805. doi:10.1097/AUD.0b013e318294e3d2
99. Lim LJZ, Dennis DL, Govender S, Colebatch JG. Differential effects of duration for ocular and cervical vestibular evoked myogenic potentials evoked by air- and bone-conducted stimuli. *Exp Brain Res* (2013) 224:437–45. doi:10.1007/s00221-012-3323-1
100. Pelosi S, Schuster D, Jacobson GP, Carlson ML, Haynes DS, Bennett ML, et al. Clinical characteristics associated with isolated unilateral utricular dysfunction. *Am J Otolaryngol* (2013) 34:490–5. doi:10.1016/j.amjoto.2013.04.008

Conflict of Interest Statement: IC is an unpaid consultant to Otometrics, but has received support from Otometrics for travel and attendance at conferences and workshops. For the remaining authors the research was conducted in the absence of any commercial or financial relationships that could be construed as a potential conflict of interest.

Copyright © 2018 Curthoys, Grant, Burgess, Pastras, Brown and Manzari. This is an open-access article distributed under the terms of the Creative Commons Attribution License (CC BY). The use, distribution or reproduction in other forums is permitted, provided the original author(s) and the copyright owner are credited and that the original publication in this journal is cited, in accordance with accepted academic practice. No use, distribution or reproduction is permitted which does not comply with these terms.